19

High-Sensitivity Detection of Bioluminescence at an Optical Fiber End for an ATP Sensor

Masataka Iinuma, Yasuyuki Ushio, Akio Kuroda and Yutaka Kadoya
Graduate School of Advanced Sciences of Matter, Hiroshima University
Japan

1. Introduction

In biological studies, the luminescence from fluorescent proteins or luminescent enzymes is widely used for monitoring a change of environment at a cell. Biomolecules used for this probing, such as Green Fluorescence Protein(GFP) or luciferase molecules can respond to the existence of specific molecules or ions and subsequently emit a photon. The detection of a specific molecule can then be confirmed by detecting the emitted photons efficiently with a photon detector. A highly efficient detection of the luminescence is normally essential to a high sensitivity to the specific molecules or ions. An improvement of the sensitivity can upgrade the capability of detection in a low concentration of sample solution. Therefore, there are many efforts to improve the efficiency of the collection of emitted photons and of the optical coupling to the photon detector (Yotter, 2004).

A straightforward approach is to directly detect the luminescence from the whole sample solution in a test tube as shown in Fig. 1 (a). However, to realize high efficiency detection, this method needs a single photon detector with a wide photon-sensitive area, which is ideally larger than the photon-emission area in the test tube. The reason is that it is difficult to image incoherent light such as natural light to a smaller area than the emission area. Here, we are introducing an alternative method, where the luminescent biomolecules are immobilized at an optical fiber end and the luminescence is detected by a photon detector which is optically coupled to the other optical fiber end. The sketch of the optical fiber-based systems is shown in Fig. 1 (b). This method has been investigated for application to a fiberoptic biosensor, which is constructed by immobilizing either an enzyme or an antibody. A review is given in (Arnold, 1991), (Blum & Gautier, 1991).

This method has three merits. The first one is to permit a local detection within the sample solution, because the optical fiber end functions as a needle-like probe in the solution. The second one is that the detection scheme does not require that the photon detector is very close to the sample solution. This feature makes it easier to mount the sensing parts in integrated bioengineering, such as μ-TAS. The third merit is that single photon detectors with a small sensitive area can be used, because the photon-emission area, which is almost identical to the cross section of the core part in the optical fiber, is small. In general, single photon detectors have lower dark counts for smaller sensitive area. Low dark counts are very significant, because it essentially gives the upper limit of the sensitivity of photon detection. Recently, single photon detectors using avalanche photodiodes (APDs) have become widely available with good performance, but their sensitive area is small and has a typical size of 0.1 mm. The

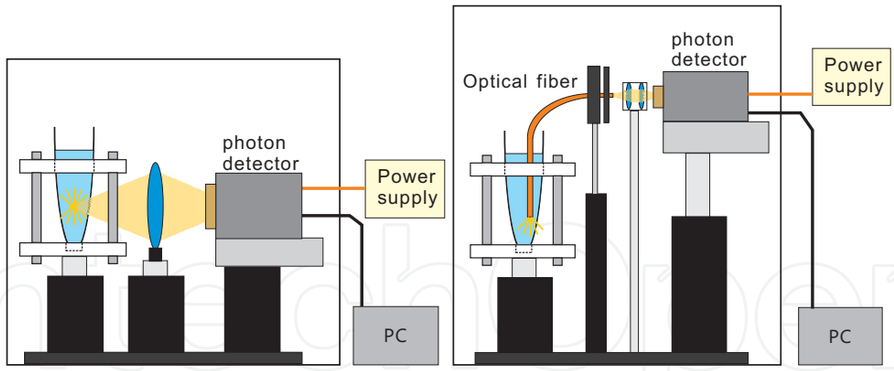

(a) Direct detection system (b) Optical fiber-based detection system

Fig. 1. Schematic figure of two detection systems

luminescence detection by the optical fiber-based system allows us to fully use the merits of compactness, high quantum efficiency, and low noise of these APD detectors.

We have built a detection system of bioluminescence at an optical fiber end and investigated the sensitivity of Adenosine triphosphate (ATP) detection by using an APD-type photon detector (Iinuma et al., 2009). ATP is a good indicator of biochemical reaction or life activity, since ATP is considered as the universal currency of biological energy for all living things. Therefore, there are a lot of efforts to develop ATP-sensing techniques for compact and efficient ATP detection (Stanley, 1992), (Andreotti & Berthold, 1999), (Gourine et al., 2005). In particular, high-sensitivity detection of ATP can indicate the existence of microorganisms even in low numbers. Thus, a compact and simple detection system with extremely high sensitivity is very desirable.

One powerful method for highly sensitive ATP detection is to use the chemical reaction involved in the bioluminescence, the luciferin-luciferase reaction (Fraga, 2008). In this reaction, after one ATP molecule and one luciferin molecule are bound to one luciferase molecule, the luciferin molecule is oxidized using the energy of ATP. As a consequence, one photon is emitted during the transition from the excited state to the ground state of the oxidized luciferin molecule bound to the luciferase molecule. The emission of one photon indicates the use of the energy of one ATP molecule. In the method using the luciferin-luciferase reaction, the efficient detection of the bioluminescence is essential for high-sensitivity detection of ATP.

Since the oxidation of luciferin is catalyzed by the enzyme luciferase, the immobilization of luciferase molcules on solid probes of various sizes allows highly sensitive and local measurements of ATP. Three types of immobilization have been used: firstly attachment to the cell surface (Nakamura et al., 2006), secondly attachment to small particles, such as nanoparticles (Konno et al., 2006) and glass beads (Lee et al., 1977), thirdly attachment to extended objects with a size in the centimeter range, such as strips (Blum et al., 1984), (Ribeiro et al., 1998) and films (Worsfold & Nabi, 1986). For the ATP-detection on an intermediate scale below 1 millimeter, a fiberoptic probe employing immobilized luciferase (Blum & Gautier, 1991) as well as microchips (Tanii et al., 2001), (Tsuboi et al., 2007), can be utilized. The detection system of bioluminescence at an optical fiber end can achieve local detection of ATP within the sample solution. Realization of high sensitivity potentially provides the local detection of extremely low number of microorganisms. Thus, it is desirable

to construct a highly efficient detection system of the bioluminescence at an optical fiber end and to evaluate the detection limit with the system.

The rest of this chapter is organized as follows. In sec. 2, we describe a concept for the construction of the optical fiber-based system for efficient detection of a fluorescence at the optical fiber end. In sec. 3, we show how to optimize the parameters of the optical fiber and the coupling optics so as to realize high photon-collection efficiency. In sec. 4, we describe the application of the constructed detection system to ATP sensing. By immobilizing luciferase molecules at the optical fiber end, the bioluminescence by luciferin-luciferase reaction can be detected using the optical fiber-based system. We evaluated the sensitivity of ATP with this system. Sec. 5 summarizes present results and problems.

2. General concept for construction of the optical fiber-based system

For a luminescence detection system using an optical fiber with a core diameter ϕ_0 and a numerical aperture NA_0, a collection efficiency of the luminescence η at the optical fiber end depends only on NA_0 as shown in Fig. 2. From a simple calculation based on the solid angle

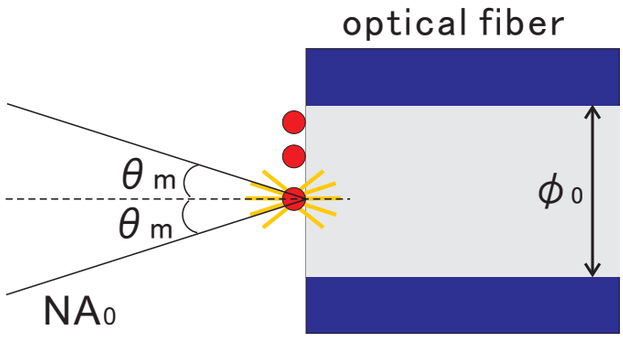

Fig. 2. Fluorescence at the optical fiber end. θ_m is a maximum opening angle for light propagation in the optical fiber.

with a maximum opening angle θ_m, $\eta(NA_0)$ can be expressed as,

$$\begin{aligned}\eta\left(NA_0\right) &= \frac{1}{2}\left(1-\cos\theta_m\right) \\ &= \frac{1}{2}\left[1-\sqrt{1-\left(\frac{NA_0}{n_w}\right)}\right],\end{aligned} \tag{1}$$

where n_w is the refraction index of the substance surrounding the optical fiber end. In immersing the optical fiber end into water, its value should be identical to the value of water, which is about 1.33. Fig. 3 shows the calculated values of the collection efficiency $\eta(NA_0)$ as a function of NA_0 using Eq. (1) at $n_w = 1.33$. One can easily see that $\eta(NA_0)$ increases with NA_0.

In the following, let us consider the situation where the other optical fiber end is optically coupled to a photon detector with a circular sensitive area having a diameter ϕ_3 and a numerical aperture NA_3. The coupling efficiency ϵ between the optical fiber end and the photon detector depends on ϕ_0, NA_0 of the optical fiber and ϕ_3, NA_3 of the photon detector

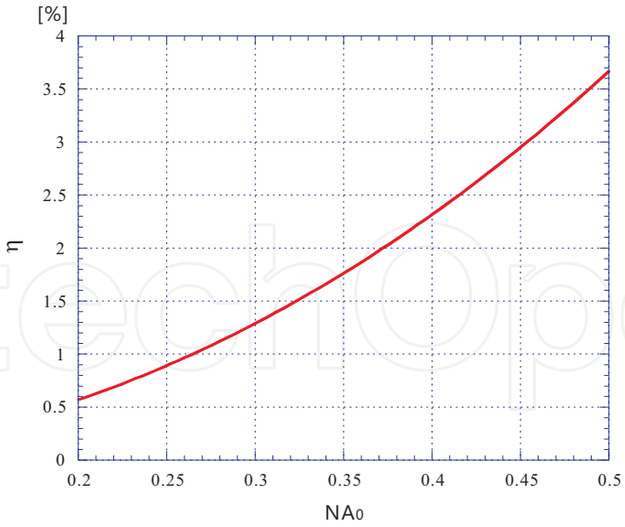

Fig. 3. Calculated values of collection efficiency as a function of NA_0 at n_w=1.33

used. Since the number of emitted photons is proportional to the square of ϕ_0 and $\eta(NA_0)$ increases with NA_0 as expressed by Eq. (1), the number of transmitted photons to the other optical fiber end is proportional to the square of ϕ_0 and $\eta(NA_0)$. On the other hand, the coupling efficiency ϵ generally decreases as ϕ_0 or NA_0 increases. Thus, we can define the following formula for a figure of merit (FOM) and optimize ϕ_0, NA_0 and parameters of the coupling optics x_i to maximize this FOM:

$$FOM = \phi_0^2 \cdot \eta(NA_0) \cdot \epsilon(\phi_0, NA_0, x_i; \phi_3, NA_3) \tag{2}$$

It should be noted that ϵ can ideally be 100 % under the conditions of $\phi_0 \leq \phi_3$ and $NA_0 \leq NA_3$. In many cases, the condition $NA_0 \leq NA_3$ is satisfied when using typical photon detectors. Thus, under the condition of $NA_0 \leq NA_3$, we can classify two cases: case (1) is $\phi_0 \leq \phi_3$ and case (2) is $\phi_0 > \phi_3$. In case (1), ϵ is constant and can ideally be 100 % and the total detection efficiency is limited only by $\eta(NA_0)$. Therefore, optimization of the coupling optics is not necessary. The conditions $\phi_0 = \phi_3$ and $NA_0 = NA_3$ both maximize the FOM and the sensitivity becomes highest. In case (2), however, the optimization of ϕ_0, NA_0, and the parameters x_i for a design of the coupling optics are necessary for given values of NA_3 and ϕ_3, because ϵ decreases as ϕ_0 or NA_0 increases.

3. Design of coupling optics

3.1 Photon detectors

Photon detectors generally have two significant factors contributing to the sensitivity of detection for weak light: the efficiency and the dark counts of the photodetector. A cooled APD which can detect for single photons is mostly used because of its very low dark counts. The sensitive area must be very small for realizing a large reduction of the dark counts, but the quantum efficiency is several times larger than that of a photomultiplier tube(PMT). Furthermore, the APD has the useful characteristics of compactness, easy operation, and durability in comparison with a PMT. To construct an optical fiber-based system with high

sensitivity, we chose an APD-type photon counting module (SPCM-AQR-14) manufactured by Perkin Elmer Co. Ltd., which has a quantum efficiency η_{qe} of 55 % at 550 nm and dark counts of about 100 s^{-1}. The APD has a circular sensitive area, where ϕ_3 is 0.175 mm and NA_3 is 0.78, as calculated from the geometrical structure between the sensitive area and the photon detection window. If we use an optical fiber with $\phi_0 > \phi_3$ to increase the number of emitted photons, it is necessary to optimize ϕ_0, NA_0, and to design the coupling optics for maximal sensitivity.

3.2 Design concept and procedure

We can consider the coupling optics between the optical fiber end and the APD as an optical system imaging a light source with NA_0 and ϕ_0 onto the APD with NA_3 and ϕ_3. The basic design of the coupling optics is shown in Fig. 4.

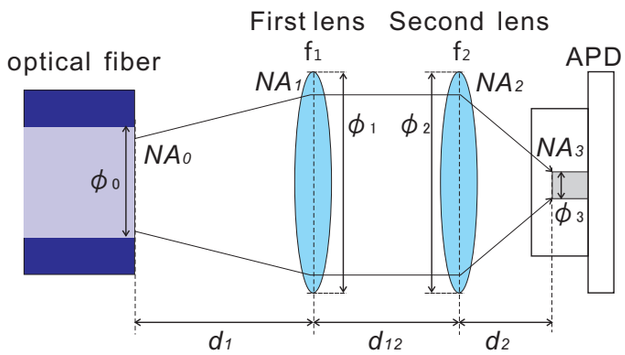

Fig. 4. Design of the coupling optics between the fiber output and the APD

Among the parameters shown in Fig. 4, we firstly determine the parameters of optical components, the focal length f_1 and the numerical aperture NA_1 of the first lens, the focal length f_2 and the numerical aperture NA_2 of the second lens, and the distance d_{12} between the first lens and the second lens. The second lens is selected among available lenses to make NA_2 as large as possible while staying below NA_3. We also select the first lens among available lenses to make NA_1 as large as possible while staying below NA_2. As the result, f_1, NA_1, f_2, NA_2 were determined as shown in Table 1.

	focal length	NA	diameter
first lens	8.0 mm	0.50	8.68 mm
second lens	3.1 mm	0.68	5.1 mm
APD sensitive area		0.78	0.175 mm

Table 1. Parameters of optical components

Taking into account of geometrical structure of lens mounts and fixing both of the first and second lens, the distance d_{12} should be longer than 3 mm. In this case, we determined $d_{12} = 5$ mm. The remaining parameters in this optical system were NA_0, ϕ_0, the distance d_1 between the fiber end and the first lens, and the distance d_2 between the second lens and the APD. These parameters can be determined in two steps as follows. In the first step, NA_0 and ϕ_0 are optimized to maximize the FOM expressed as Eq. (2) under the conditions $f_1 = d_1$ and $f_2 = d_2$. In the second step, d_1 and d_2 are optimized to maximize $\epsilon(d_1, d_2, \phi_0, NA_0)$ for given values of NA_0 and ϕ_0 obtained in the first step.

3.3 Determination of parameters in the optical system

The optimization procedure requires specific values of $\eta(NA_0)$ and $\epsilon(NA_0, \phi_0)$ for obtaining the FOM. Since the values of $\eta(NA_0)$ were given from Eq. (1) as shown in Fig. 3, it is necessary to calculate the values of $\epsilon(NA_0, \phi_0)$ at $d_1 = f_1$ and $d_2 = f_2$. The simple method for obtaining the efficiency is a statistical simulation by ray tracing.

The optical fiber end can be considered as a light source with ϕ_0 and NA_0. To calculate the efficiency, an event of light emission is randomly generated at an arbitrary position within ϕ_0 and at an arbitrary direction within NA_0. Subsequently, the final state of light at the APD sensitive area is calculated by the transformation of the initial state based on ray tracing. We repeat a procedure containing the generation of one event in the light emission and the subsequent transformation to the final state at the APD via intermediate states at the first lens and the second lens, and count the number of the events, where the conditions at the first lens NA_1, ϕ_1, at the second lens NA_2, ϕ_2, and at the APD NA_3 and ϕ_3 are all fulfilled. The efficiency can be obtained as the ratio of number of counts to the total number of event generation.

The propagation of light can be described with matrix formalism in paraxial optics (Yariv, 1997). The light at the initial state (r_i, r_i'), where r_i is a distance from an optical axis of optics and r_i' is a slope of the light direction, can be transferred by the following matrices, for example,

$$M_{free} = \begin{bmatrix} 1 & d \\ 0 & 1 \end{bmatrix}$$

$$M_{lens} = \begin{bmatrix} 1 & 0 \\ -\frac{1}{f} & 1 \end{bmatrix},$$

where M_{free} is the transfer matrix of free-space propagation far from the distance d and M_{lens} is the transfer matrix of thin lens with the focal length f. Any state of light expressed as the vector form (r, r') can be transferred by any combination of the transfer matrices. Therefore, the transfer matrix $M_{coupling}$ describing the optical system shown in Fig. 4 can be expressed as follows,

$$M_{coupling} = \begin{bmatrix} 1 & d_2 \\ 0 & 1 \end{bmatrix} \cdot \begin{bmatrix} 1 & 0 \\ -\frac{1}{f_2} & 1 \end{bmatrix} \cdot \begin{bmatrix} 1 & d_{12} \\ 0 & 1 \end{bmatrix} \cdot \begin{bmatrix} 1 & 0 \\ -\frac{1}{f_1} & 1 \end{bmatrix} \cdot \begin{bmatrix} 1 & d_1 \\ 0 & 1 \end{bmatrix}$$

$M_{coupling}$ can transfer the initial state (r_i, r_i') at the optical fiber end to the final state (r_f, r_f') at the APD sensitive area.

Thus, the values of ϵ were obtained by the statistical method with the transfer matrix $M_{coupling}$, where random numbers for setting initial states were generated with the software package based on algorithm of Mersenne Twister (Matsumoto & Nishimura, 1998). The calculated results are shown as a function of NA_0 in Fig. 5.

Fig. 5 shows that ϵ is decreasing with increasing NA_0 and ϕ_0. As a consequence, ϵ becomes 100 % at $\phi_0 = 0.4$ mm and $NA_0 \leq 0.25$. However, the reduction of ϕ_0 and NA_0 makes both η

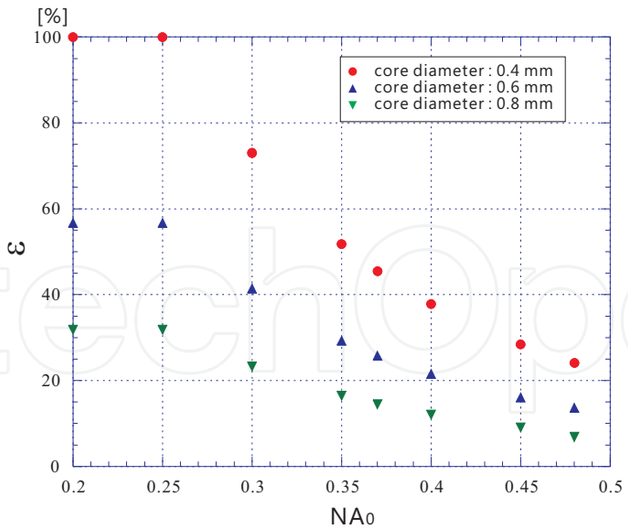

Fig. 5. Calculated values of coupling efficiency ϵ as a function of NA_0. The solid circles indicate the values at $\phi_0 = 0.4$ mm, the solid triangles are the values at $\phi_0 = 0.6$ mm, and the solid inverse triangles are the values at $\phi_0 = 0.8$ mm.

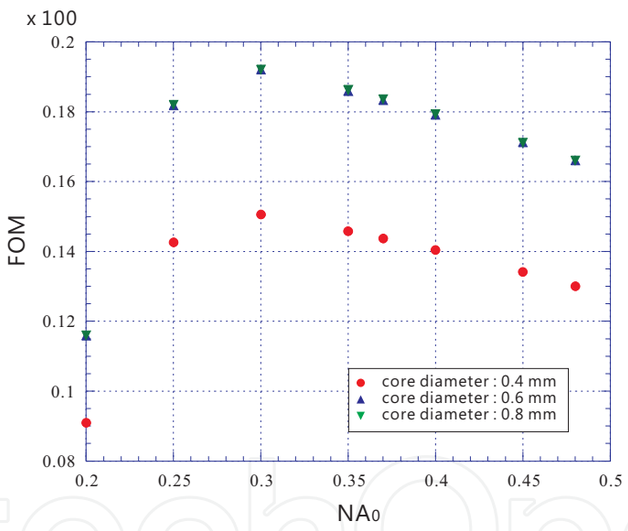

Fig. 6. Calculated values of FOM as a fuction of NA_0. The solid circles indicate the values at $\phi_0 = 0.4$ mm, the solid triangles are the values at $\phi_0 = 0.6$ mm, and the solid inverse triangles are the values at $\phi_0 = 0.8$ mm.

and the number of emitted photons smaller. Therefore, the calculation of the FOM is necessary for the optimization of NA_0 and ϕ_0.

The plot of the FOM as a function of NA_0 is shown in Fig. 6. One can easliy see that the FOM is maximal at $NA_0 = 3.0$. In addtion, the value of the FOM for $\phi_0 = 0.6$ mm is almost same as the one for $\phi_0 = 0.8$ mm. This means that the FOM is saturated for larger diameters than $\phi_0 = 0.6$ mm because the size of the transferred image at the APD is larger than the APD sensitive area.

Optical fibers with $NA_0 = 3.0$ are not easily obtainable, whereas optical fibers with $NA_0 = 2.5$ and $NA_0 = 3.7$ are readily available. Fig. 6 shows that the slope above $NA_0 = 3.0$ is flatter than the one below. In the upper part, the misalignment or imperfection of the optical system has less influence on the coupling efficiency. Therefore, we selected $\phi_0 = 0.6$ mm and $NA_0 = 3.7$.

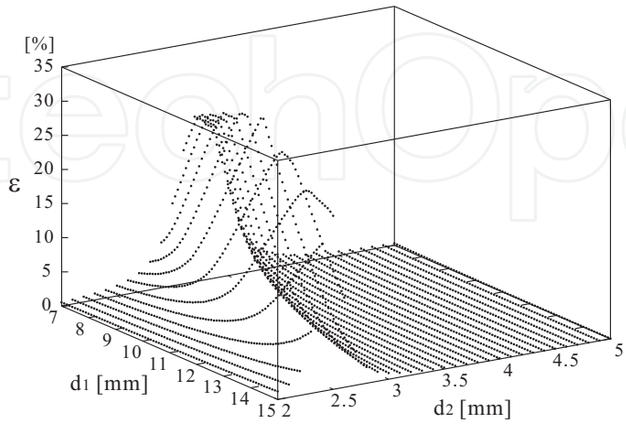

Fig. 7. Calculated values of ϵ as fuctions of d_1 and d_2 for given values of $NA_0 = 0.37$ and $\phi_0 = 0.6$ [mm].

In a second step, d_1 and d_2 were optimized to maximize $\epsilon(d_1, d_2)$ for $NA_0 = 0.37$ and $\phi_0 = 0.6$ mm. Fig. 7 shows the calculated values of ϵ as functions of d_1 and d_2. From the peak of ϵ in Fig. 7, the results of $d_1 = 11.6$ mm and $d_2 = 2.7$ mm were obtained for $NA_0 = 0.37$ and $\phi_0 = 0.6$. These parameters provide the maximum $\epsilon(d_1, d_2)$ of 33.33 %, $\eta(NA_0)$ of 1.95 % and FOM $\times 100$ is 0.234 which value is higher than the maximum in Fig. 6.

4. Application to the ATP sensing system

4.1 Luciferin-luciferase reaction

Bioluminescence in living organisms, such as fireflies and some marine bacteria, typically occurs due to the optical transition from the excited state to the ground state of oxidized luciferin molecules produced by the luciferin-luciferase reaction under the catalytic activity of luciferase molecules. This reaction can be expressed by the following sequence of reaction steps:

$$\begin{aligned} &\mathrm{E} + \mathrm{LH_2} + \mathrm{S} \rightleftharpoons \mathrm{C} + \mathrm{PP_i} \\ &\mathrm{C} + \mathrm{O_2} \rightarrow \mathrm{E} + \mathrm{P^*} + \mathrm{AMP} + \mathrm{CO_2} \\ &\mathrm{P^*} \rightarrow \mathrm{P} + \gamma \end{aligned}$$

where E indicates luciferase, LH_2 luciferin, PP_i pyrophoric acid, C is an enzyme-substrate compound $E \cdot LH_2$-AMP, AMP adenosine monophosphate, P oxidized luciferin, and γ a photon (DeLuca, 1976). The emission of one photon at the position of luciferase molecule indicates the use of the energy of one ATP molecule.

The immobilization of luciferase molecules at the optical fiber end enables us to sense the presence of ATP around the fiber end using single photon detection. For this purpose, we used a compound protein containing a silica-binding protein (SBP) molecule and a luciferase

molecule (SBP-luciferase), which were recently synthesized by Taniguchi and co-workers (Taniguchi et al., 2007). This protein makes it possible to immobilize a luciferase molecule on the optical fiber end via a SBP molecule while retaining its activity. The spectrum of the emitted photons shows a central wavelength of 550 nm and a width of about 100 nm (Denburg et al., 1969), (Ugarova & Brovko, 2002). Since the APD module has the large quantum efficiency for the photons from the luciferin-luciferase reaction, the APD photon counting module is suitable for ATP sensing.

4.2 Reaction-diffusion differential equation

Fig. 8 shows the enzyme reaction which describes the sequence of reactions.

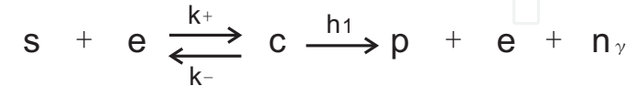

s : ATP (S)
e : luciferaze (E)
p : oxyluciferin (P)
n_γ : photon (γ)
c : E · LH_2-AMP
k_+, k_- : kinetic constants
h_1 : reaction constant

Fig. 8. Enzyme reaction describing luciferin-luciferase reaction

Here, s, e, c, p, n_γ in Fig. 8 represents a concentration of ATP, luciferase, E · LH_2-AMP, oxidized luciferin, and emitted photon, respectively. In addition, k_+, k_- are kinetic constants for equilibrium and h_1 is a reaction constant.

In a solution containing nonlocalized homogeneously dispersed luciferase and ATP, the Michaelis-Menten theory can be simply applied to the above reaction. In the presence of enough luciferin molecules in the solution, a rate of emitted photons at steady state v_γ can be expressed as the Michaelis-Menten formula,

$$v_\gamma = \frac{V_0 S}{S + K_M}, \tag{3}$$

where V_0 is a maximum reaction rate which is equivalent to a product of the number of luciferase molecule and h_1, K_M is the Michaels constant expressed as $K_M = \frac{k_- + h_1}{k_+}$ and S is the ATP concentration.

In the fiber-based system for sensing dispersed ATP molecules, on the other hands, an ATP-flow generated by a gradient of ATP concentration around the luciferase-terminated fiber end carries ATP molecules to the vicinity of immobilized SBP-luciferase molecules. The ATP molecule is bound to the immobilized SBP-luciferase molecule near them and subsequently contributes the luciferin-luciferase reaction at this fiber end. To calculate the rate of emitted photons, therefore, it is necessary to consider not only a reaction rate but also an ATP diffusion rate.

The series of reaction-diffusion equations describing the enzyme reaction shown in Fig. 8 can be expressed as,

$$\begin{aligned}
\frac{ds}{dt} &= D\left(\frac{\partial^2 s}{\partial x^2} + \frac{\partial^2 s}{\partial y^2}\right) + R(s,e,c) \\
\frac{de}{dt} &= -k_+ se + k_- c + h_1 c \\
\frac{dc}{dt} &= k_+ se - k_- c - h_1 c \\
\frac{dn_\gamma}{dt} &= h_1 c,
\end{aligned} \tag{4}$$

where D is a diffusion constant of ATP in water and $R(s,e,c)$ is expressed as follows.

$$R(s,e,c) \equiv \begin{cases} -k_+ se + k_- c & (x,y \in \Gamma_{fiber}) \\ 0 & (\text{otherwise}) \end{cases}$$

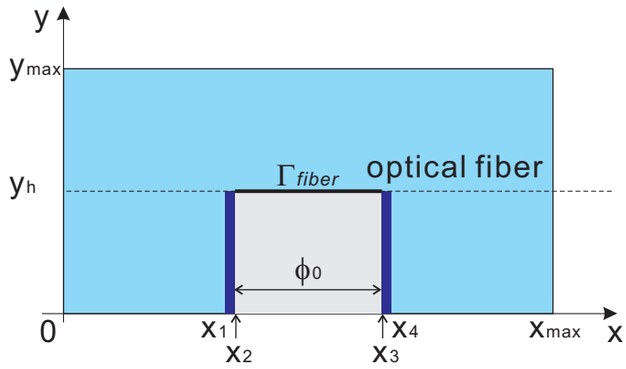

Fig. 9. Coordinate system of x and y around the fiber end.

Fig. 9 shows the definition of the coordinate system of x and y . Here, it should be noted that $s(x,y,t)$ is a function of x, y, t and $e(t)$ and $c(t)$ are functions of only t. Γ_{fiber} is defined as an area where the reaction occurs and equivalent to the core part ϕ_0 in the optical fiber. In this coordinate system, it can be represented as the interval of $x_2 \leq x \leq x_3$ with $y = y_h$. The both intervals of $x_1 \leq x \leq x_2$ and $x_3 \leq x \leq x_4$ with $y = y_h$ represent the parts of clad in the optical fiber.

By dividing the space around the fiber end into finite spatial steps and also dividing the time into finite time steps, we can numerically solve the series of reaction-diffusion equation Eq. (4) under the boundary conditions presented in Table 2. Here, s_0 in Table 2 is an initial ATP concentration that should be uniform into the whole solution before starting the reaction. The numerical solutions can be given as time evolution of spatial distribution of concentration $s(x_i, y_i, t_i)$, $e(t_i)$, and $c(t_i)$ and the rate of emitted photons can be obtained from $h_1 c(t_i)$. The peak of the photon-emission rate in time corresponds to the reaction rate given by the Michaelis-Menten formula.

In order to check the possibility that the emission rates are limited by the diffusion rate of ATP, we numerically obtained the peak values of the photon-emission rate at various ATP concentration and compared to the reaction rate calculated by Michaelis-Menten formula. To obtain numerical solutions at each time step, spatial segmented equations derived from Eq.

region	$x = 0$	$0 \leq x < x_1$ $y = 0$	$x = x_1$ $0 \leq y < y_h$	$x_1 \leq x < x_2$ $y = y_h$	$x_2 \leq x \leq x_3$ $y = y_h$
condition	$s = s_0$	$s = s_0$	$\left.\frac{ds}{dx}\right\|_{x=x_1} = 0$	$\left.\frac{ds}{dy}\right\|_{y=y_h} = 0$	$\left.\frac{ds}{dy}\right\|_{y=y_h} = 0$
region	$x_3 < x \leq x_4$ $y = y_h$	$x = x_4$ $0 \leq y < y_h$	$x_4 < x \leq x_{max}$ $y = 0$	$x = x_{max}$	$y = y_{max}$
condition	$\left.\frac{ds}{dy}\right\|_{y=y_h} = 0$	$\left.\frac{ds}{dx}\right\|_{x=x_4} = 0$	$s = s_0$	$s = s_0$	$s = s_0$

Table 2. boundary conditions for solving Eq. (4). s_0 is the initial ATP concentration.

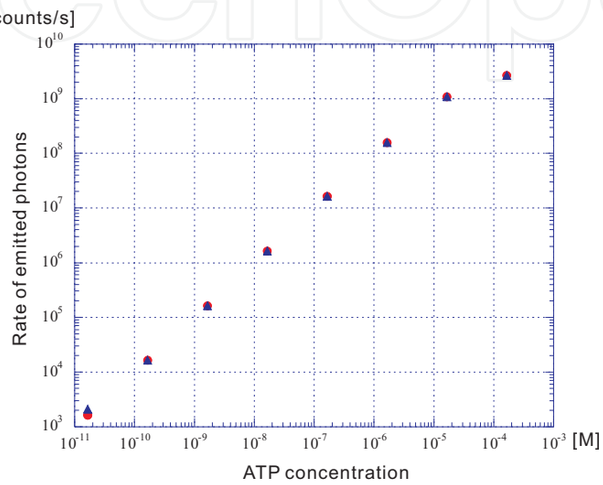

Fig. 10. Comparison of the results calculated from numerical solutions of reaction-diffusion equations to the results of Michaelis-Menten formula. Closed triangles indicate values of ATP diffusion process using typical values of kinetic constants, closed circles are values given by Michaelis-Menten formula.

(4) were solved in terms of time using the software package of ordinary differential equations DASKR (Brown et al., 1998), where the ATP diffusion constant was $D = 0.5 \times 10^{-5}$ cm^2/s (Aflao & DeLuca, 1987), the geometrical parameters were $x_{max} = 1.4$ mm, $y_{max} = 2$ mm, $y_h = 1$ mm, $x_1 = 0.38$ mm, $x_4 = 1.02$ mm, the kinetic constants were $k_+ = 20000$ M^{-1}s^{-1}, which was estimated from the typical buildup time of 0.3 s (DeLuca & McElory, 1974), and $k_- = 0.515$ s^{-1}, which was calculated with the relational form $K_M \cdot k_+ - h_1$. As other parameters, we used $h_1 = 0.125$ s^{-1} (Branchini et al., 2001), $K_M = 3.2 \times 10^{-5}$ M, and the surface density of luciferase molecule $\sigma_0 = 9.03 \times 10^{10}$ mm^{-2} (Taniguchi et al., 2007), which were also used for Michaelis-Menten formula. The Michaelis constants $K_M = 3.2 \times 10^{-5}$ M was obtained from data analysis of counts of detected photons, which describes in Sec. 4.

Fig. 10 shows the results of two kinds of calculations. The closed triangles indicate the values obtained from numerical solutions of Eq. (4), whereas the closed circles are the values deduced from Michaelis-Menten formula. The results of ATP diffusion process have good agreements with ones given by the Michaelis-Menten theory. Therefore, we can conclude that the ATP diffusion is not a rate-limiting process for the present rate of the chemical reaction.

4.3 Measurement of the sensitivity

4.3.1 Immobilization of luciferase

Before immobilizing the luciferase molecules, we cut optical fiber and cleaned the cut surface with ethanol and Tris buffer (0.25 mM Tris-HCl with 0.15 M NaCl). After cleaning, the surface was immersed in a solution of SBP-luciferase and was left at a temperature of 3°C to 6°C for a period of about two hours.

4.3.2 Sample solutions

The samples were a 1:4:4:31 mixture of 20 mM D-luciferin solution, Tris buffer solution(250 mM Tris-HCl mixed with 50 mM $MgCl_2$), ATP solution, and distilled water. Several solutions of ATP with different ATP concentrations were made by diluting the ATP standard in ATP Bioluminescence Assay Kit CLS II manufactured by Roche Co. Ltd. Thus, a series of sample solutions with different ATP concentrations were prepared in advance. An additional sample without ATP was also produced by mixing distilled water instead of the ATP solution. This sample was measured in order to obtain a background before the ATP measurements.

4.3.3 Data taking system

TTL pulses outputted from the APD photon counting module were counted by a PC card installed in a personal computer(PC). The number of pulses occurring during 10 s were recorded every 10 s by the PC

4.3.4 Results

The time dependence of photon counts per 10-s interval were measured after the luciferase-terminated end were immersed in the sample solutions with various ATP concentration. The results for 100 $\mu\ell$ solution from 1.65×10^{-4} M to 1.65×10^{-9} are shown in Fig. 11.

The photon counts increase and reach a maximum at about 150 s after immersion. Then, they decrease very slowly to the background level. Therefore, for obtaining high sensitivity, it is practical to continue the measurement for about 300 s after the luciferase-terminated end is immersed in the solution. A background level of approximately 120 s^{-1} was determined as an average of counts for background data. It was found to correspond well to the dark counts of the photon counting module.

ATP concentration	integrated counts	BG-subtracted counts	statistical errors
no ATP (background)	34490		
1.65×10^{-11} M	34664	174	262.97
1.65×10^{-10} M	35346	856	264.27
1.65×10^{-9} M	46770	12280	285.06
1.65×10^{-8} M	139300	104810	416.88

Table 3. Integrated counts for ATP sample solutions

Table 3 presents integrated counts of detected photons during 300 s from the origin of time. Statistical errors are estimated as one standard deviation assuming Poisson distribution. From Table 3, the sensitivity in this optical fiber-based system is limited to 1.65×10^{-10} M, which

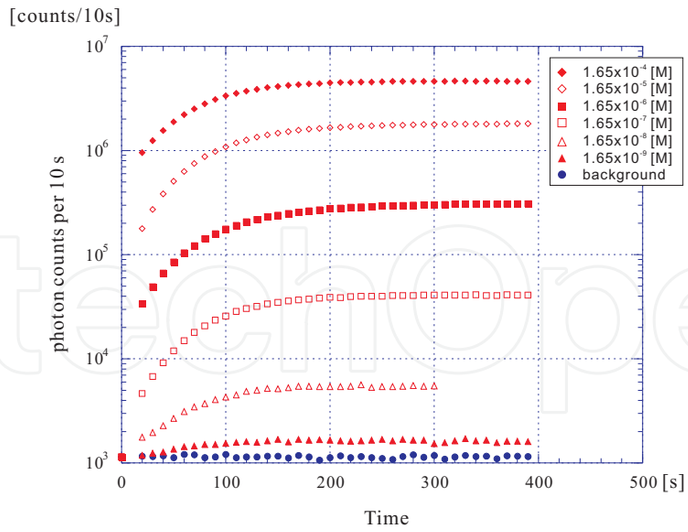

Fig. 11. Measured photon counts per 10 s as a function of time at ATP concentration 1.65×10^{-4} M, 1.65×10^{-5} M, 1.65×10^{-6} M, 1.65×10^{-7} M, 1.65×10^{-8} M, 1.65×10^{-9} M, which are represented by closed diamonds, open diamonds, closed squares, open squares, open triangles, closed triangles, respectively. Closed circles indicate background counts.

corresponds to a number of ATP molecules of about 10^{-14} mol in the 100 $\mu\ell$ solution. We also ascertained that our system is sensitive to the 10^{-10} M level even with a $10\mu\ell$ solution, in which the absolute ATP concentration is 10^{-15} mol.

In order to check the ATP concentration dependence of the photon counting rate at maximum, the average of counts in six 10-s intervals around the time at which the counting rate became maximal was calculated for each ATP concentration. The results are indicated by solid circles in Fig. 12. This figure shows that the lower limit of the sensitivity is 1.65×10^{-9} M taking into account of statistical errors. If the statistical errors reduce to half of the present ones, which means that statistics at each point becomes four times as large as 60-s interval, the detection of 1.65×10^{-10} M also becomes feasible. This is consistent with the results presented in Table 3. The analysis of fitting data points in Fig. 12 provided the Michaelis constant of 3.2×10^{-5} M.

4.3.5 Discussion

In Fig. 12, the open squares show predictions of the counting rate estimated from the results of numerical solutions shown in Fig. 10 with the total detection efficiency in our detection system, which can be expressed as $\epsilon_{total} = \eta \cdot \epsilon \cdot \eta_{qe}$. Its value was calculated to be 0.00354 for photons with the wavelength 550 nm. Comparing the experimental data with the predictions, there are disagreements amounting to roughly one order of magnitude.

The results suggest the ATP diffusion does not limit the detection limit. Therefore, the possible reasons for the discrepancies may be the following.

(1) The rate of the chemical reaction per luciferase molecule itself becomes small.
(2) The number of immobilized active molecules is lower than expected.

We have also confirmed that the buildup time in Fig. 11 is about 30 times longer than that in a solution containing only nonlocalized homogeneously dispersed SBP-luciferase

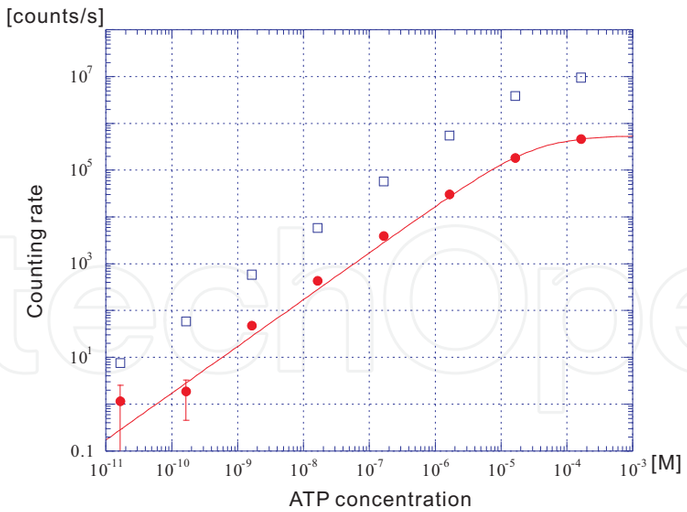

Fig. 12. Measured photon counting rate as a function of ATP concentration. Solid line is a curve obtained by fitting data with the Michaelis-Menten formula. Open squares are values estimated from the results of numerical solutions shown in Fig. 10 with total detection efficiency $\epsilon_{total} = 0.00354$.

molecules. There are also other experimental results claiming the decrease in acitivity of immobilized luciferase moleclues (Nishiyama et al., 2008), (Tanaka et al., 2011). The reason of this discrepancy is still an open question. These results suggest that it will be necessary to study the reaction at the end of the optical fiber in more detail in order to improve the sensitivity.

5. Summary

We introduced a method of high-sensitivity detection of bioluminescence at an optical fiber end for an ATP sensor as an efficient alternative to direct detection of bioluminescence from a sample solution. For efficiently detection of the bioluminescence, we have constructed an optical fiber-based system, where the luciferase molecules are immobilized on the optical fiber end and the other end is optically coupled to an APD-type photon counting module. We have evaluated the sensitivity of the ATP detection of this system and found that the optimization of the optical coupling system and the use of the SBP-luciferase molecules provide the detection limit of 10^{-10} M, which allows us to detect the absolute ATP concentration of 10^{-15} mol with a $10\mu\ell$ solution. To improve the sensitivity, it is necessary to study the details of the reaction at luciferase-terminated end of the optical fiber.

6. Acknowledgements

We are grateful to Dr. Kazutaka Nomura for providing the SBP-luciferase molecules and Prof. Holger F. Hofmann for reading the manuscript. We also express our thanks to Dr. Tetsuya Sato, Dr. Koichiro Sadakane, and Dr. Shuhei Miyoshi for their help in setting up the experiments. This work has been partially supported by the International Project Center for Integration Research on Quantum, Information, and Life Science of Hiroshima University and the Grant-in-Aid for Scientific Research (C)(19560046) of Japanese Society for the Promotion of Science, JSPS.

7. References

Andreotti P. E. & Berthold F. (1999). Application of a new high sensitivity luminometer for industrial microbilogy and molecular biology, *Luminescence*, Vol. 14: 19-22, ISSN 15227235

Arnold M. A. (1991). Fluorophore- and Chromophore-Based Fiberoptic Biosensors, In: *Biosensor principles and applications*, Blum L. J. & Coulet P. R. (Ed.), 195-211, Marcel Dekker, 1991, ISBN 0824785460, New York

Aflao C. & DeLuca M. (1987). Continuous Monitoring of Adenosine 5′-Triphosphate in the Microenvironment of Immobilized Enzymes by Firefly Luciferase, *Biochemistry*, Vol. 26: 3913-3920, ISSN 00062960

Blum L. J.; Coulet P. R.; Gautheron D. C. (1984). Collagen Strip with Immobilized Luciferase for ATP Bioluminescent Determination, *Biotechnol. Bioeng.*, Vol. 27: 232-237, ISSN 00063592

Blum L. J.; Gautier S. M. (1991). Bioluminescence- and Chemiluminescence-Based Fiberoptic Sensors, In: *Biosensor principles and applications*, Blum L. J. & Coulet P. R. (editors), 213-247, Marcel Dekker, 1991, ISBN 0824785460, New York

Branchini B. R.; Magyar R. A.; Murtiashaw M. H.; Portier N. C. (2001). The Role of Active Site Residue Arginie 218 in Firefly Luciferase Bioluminesence, *Biochemistry*, Vol. 40: 921-925, ISSN 00062960

Brown P. N.; Hindmarsh A. C.; Petzold L. R. (1998). Consistent initial condition calculation for differential-algebraic systems, *SIAM J. Sci. Comput.*, Vol. 19: 1495-1512, ISSN 10648275. URL: http://www.netlib.org/ode/

DeLuca M. & McElory W. D. (1974). Kinetics of the Firefly Luciferase Catalyzed Reactions, *Biochemistry*, Vol. 13: 921-925, ISSN 00062960

DeLuca M. (1974). Firefly luciferase, In: *Advances in Enzymology*, Meister A. (Ed.), Vol. 44: 37-68, Wiley, 1976, ISBN 9780471591795, New York

Denburg J. L.; Lee R. T.; McElory W. D. (1969). Substrate-Binding Properties of Firefly Luciferase 1. Luciferin-binding Site, *Arch. biochem. biophys.*, Vol. 134: 381-394, ISSN 00039861

Fraga H. (2008). Firefly luminescence: A histrical perspective and recent developments, *Photochem. Photobio. Sci.*, Vol. 7: 146-158, ISSN 1474905

Gourine A. V.; Laudet E.; Dale N.; Spyer K. M. (2005). ATP is a mediator of chemosensory transduction in the central nervous system, *Nature*, Vol. 436: 108-111, ISSN 00280836

Iinuma M.; Ushio Y.; Kuroda A.; Kadoya Y. (2009). High Sensitivity Detection of ATP Using Bioluminescence at An Optical Fiber End, *Electronics and Communications in Japan*, Vol. 92: 53-59, ISSN 03854221

Konno T.; Ito T.; Takai M.; Ishihara K. (2006). Enzymatic photochemical sensing using luciferase-immobilized polymer nanoparticles covered with artificial cell membrane, *J. Biometer. Sci. Polymer. Edn.*, Vol. 17: 1347-1357, ISSN 09205063

Lee Y.; Jablonski I.; DeLuca M. (1977). Immobilization of Firefly Luciferase on Glass Rods: Properties of the Immobilized Enzyme, *Anal. Biochem.*, Vol. 80: 496-501, ISSN 00032697

Matsumoto M. & Nishimura T. (1998). Mersenne Twister: A 623-dimensionally equidistributed uniform pseudorandom number generator, *ACM Trans. model. comput. simul.*, Vol. 8: 3-30, ISSN 10493301. URL: http://www.math.sci.hiroshima-u.ac.jp/ m-mat/MT/emt.html

Nakamura M.; Mie M.; Funabashi H.; Yamamoto K.; Ando J; Kobatake E. (2006). Cell-surface-localized ATP detection with immobilized firefly luciferase, *Anal. Biochem.*, Vol. 352: 61-67, ISSN 00032697

Nishiyama K.; Watanabe T.; Hoshina T.; Ohdomari I. (2008). The main factor of the decrease in activity of luciferase on the Si surface, *Chem. Phys. Lett.*, Vol. 453: 279-282, ISSN 00092614

Ribeiro A. R.; Santos R. M.; Rosário L. M.; Gil M. H. (1998). Immobilization of Luciferase from a Firefly Lantern Extract on Glass Strips as an Alternative Strategy for Luminescent Detection of ATP, *J. Biolumin. Chemilumin.*, Vol. 13: 371-378, ISSN 08843996

Stanley P. E. (1992). A survey of more than 90 Commercially Available Luminometers and Imaging Devices for Low-light Measurements of Chemiluminescence and Bioluminescence, Including Instruments for Manual, Automatic and Specialized Operation, for HPLC, LC, GLC and Microtitre Plates, *J. Biolumin. Chemilumin.*, Vol. 7: 77-108, ISSN 08843996

Tanaka. R.; Takahama E.; Iinuma M.; Ikeda T.; Kadoya Y.; Kuroda A. (2011). Bioluminescent Reaction by Immobilized Luciferase, *IEEJ Trans. EIS*, Vol. 131: 23-28, ISSN 03854221

Taniguchi K.; Nomura K.; Hata Y.; Nishimura Y.; Asami Y.; Kuroda A. (2007). The Si-tag for immobilizing proteins on a silica surface, *Biotechnol. Bioeng.*, Vol. 96: 1023-1029, ISSN 00063592

Tanii T.; Goto T.; Iida T.; Koh-Masahara M.; Ohdomari I. (2001). Fabrication of Adenosine Triphosphate-Molecule Recognition Chip by Means of Bioluminous Enzyme Luciferase, *Jpn. J. Appl. Phys.*, Vol. 40: L1135-L1137, ISSN 00214922

Tsuboi Y.; Furuhata Y.; Kitamura N. (2007). A sensor for adenosine triphosphate fabricated by laser-induced forward transfer of luciferase onto a poly(dimethylsiloxane) microchip, *Appl. surf. sci*, Vol. 253: 8422-8427, ISSN 01694332

Ugarova N. N.; Brovko L. Y. (2002). Protein structure and bioluminescent spectra for firefly bioluminescence, *Luminescence*, Vol. 17: 321-330, ISSN 15227235

Worsfold P. J.; Nabi A. (1986). Bioluminescent assays with immobilized firefly luciferase based on flow injection analysis, *Anal. Chim. acta*, Vol. 179: 307-313, ISSN 00032670

Yariv A. (1997). *Optical Electronics in Modern Commnications Fifth Edition*, Oxford University Press, ISBN 0-19-510626-1, New York.

Yotter R. A.; Lee L. A.; Wilson D. M. (2004). Sensor Technologies for Monitoring Metabolic Activity in Single Cells - Part I: Optical Methods, *IEEE Sensors Journal*, Vol. 4: 395-411, ISSN 00032670

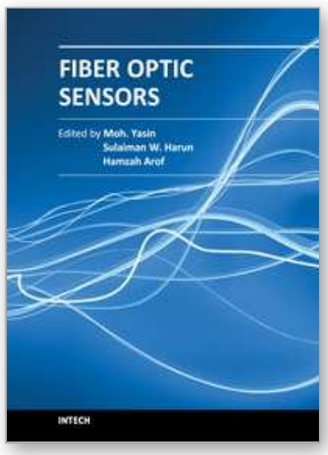

Fiber Optic Sensors

Edited by Dr Moh. Yasin

ISBN 978-953-307-922-6

Hard cover, 518 pages

Publisher InTech

Published online 22, February, 2012

Published in print edition February, 2012

This book presents a comprehensive account of recent advances and researches in fiber optic sensor technology. It consists of 21 chapters encompassing the recent progress in the subject, basic principles of various sensor types, their applications in structural health monitoring and the measurement of various physical, chemical and biological parameters. It also highlights the development of fiber optic sensors, their applications by providing various new methods for sensing and systems, and describing recent developments in fiber Bragg grating, tapered optical fiber, polymer optical fiber, long period fiber grating, reflectometry and interefometry based sensors. Edited by three scientists with a wide knowledge of the field and the community, the book brings together leading academics and practitioners in a comprehensive and incisive treatment of the subject. This is an essential reference for researchers working and teaching in optical fiber sensor technology, and for industrial users who need to be aware of current developments and new areas in optical fiber sensor devices.

How to reference

In order to correctly reference this scholarly work, feel free to copy and paste the following:

Masataka Iinuma, Yasuyuki Ushio, Akio Kuroda and Yutaka Kadoya (2012). High-Sensitivity Detection of Bioluminescence at an Optical Fiber End for an ATP Sensor, Fiber Optic Sensors, Dr Moh. Yasin (Ed.), ISBN: 978-953-307-922-6, InTech, Available from: http://www.intechopen.com/books/fiber-optic-sensors/high-sensitivity-detection-of-bioluminescence-at-an-optical-fiber-end-for-an-atp-sensor

INTECH
open science | open minds

InTech Europe
University Campus STeP Ri
Slavka Krautzeka 83/A
51000 Rijeka, Croatia
Phone: +385 (51) 770 447
Fax: +385 (51) 686 166
www.intechopen.com

InTech China
Unit 405, Office Block, Hotel Equatorial Shanghai
No.65, Yan An Road (West), Shanghai, 200040, China
中国上海市延安西路65号上海国际贵都大饭店办公楼405单元
Phone: +86-21-62489820
Fax: +86-21-62489821

IntechOpen